Effect of tempering heat treatment on mechanical properties of a medium silicon low alloy ferrite–martensite DP steel

A. Khajesarvi[1] , S. S. Ghasemi Banadkouki*[2] , S. A. Sajjadi[3]

[1,2]Department of Mining and Metallurgical Engineering, Yazd University, University Blvd, Safayieh, Yazd, PO Box: 98195 – 741, Iran

[3]Department of Materials Science and Engineering, Ferdowsi University of Mashhad, Mashhad, 91775, Iran

Abstract

This paper has been concerned to investigate in details the effect of tempering heat treatment on mechanical properties of 35CHGSA heat treatable low alloy steel under ferrite–martensite dual-phase (DP) microstructures. For this purpose, two sets of ferrite–martensite DP samples containing 6% volume fraction of ferrite have been developed using step-quench heat treatment processes at 720°C for 5 min holding times with the subsequent water quenching after being austenitized at 900°C for 15 min. In comparison to the first set of fresh ferrite–martensite DP samples (marked FDP), the finalized tempering heat treatment has been carried out at 500°C for 60 min only for the second set of tempered ferrite–martensite DP (marked TDP) samples in order to optimize the strength–ductility combination. Light and electron microscopes have been used in conjunction with hardness and tensile tests to assess the structure–property relationships of FDP and TDP heat-treated samples. The experimental results demonstrate that the mechanical properties of FDP heat-treated samples are significantly increased after tempering heat treatment. The product of tensile strength multiple total elongation has been significantly increased from 2.4 (FDP) to 15.8% GPa (TDP). Moreover, the absorbed impact energy is sharply increased from 3.5 to 12 J corresponding to the FDP and TDP marked samples, respectively. These results are rationalized to the fact that the tempering heat treatment modifies the individual mechanical behavior of ferrite and martensite microphases through influencing the ferrite and martensite hardening variations. In addition to general softening of martensite hardening from 796 to 459HV10g after tempering heat treatment, the average ferrite hardness has been surprisingly decreased from 280 (FDP-marked samples) to 207HV5g (TDP-marked samples).

Keywords: Medium silicon low alloy steel; step-quenching; tempering; ferrite–martensite DP microstructure; ferrite and martensite hardening variation.

1. Introduction

Design and development of low alloy ferrite-martensite DP steels have been one of the interesting research areas in physical metallurgy of advanced high strength low alloy steels over the past few decades ago [1-10]. Sunil et al. [8] has investigated the mechanical properties of ferrite-martensite DP steels produced through intermediate quenching technique and reporting that the formation of 50% volume fraction of martensite in conjunction with the remaining ferrite area have been associated with the optimized tensile and impact properties. Pushkareva et al. [9] have studied the relationships between microstructure, mechanical properties and damage mechanisms in high martensite containing DP steels and observed that for a constant chemical composition, the

**Corresponding author*
E-mail: sghasemi@yazd.ac.ir
Address: Department of Mining and Metallurgical Engineering, Yazd University, University Blvd, Safayieh, Yazd, PO Box: 98195 – 741, Iran
1. Ph.D. Candidate
2. Associate professor
3. Professor

ultra-high strength (UTS > 1000MPa) DP steels can be developed as the volume fraction of martensite increases in the microstructures. Movahed et al. [10] have concluded that the elongation, tensile strengths and fracture energy of a low alloy ferrite–martensite DP steel can be simultaneously increased with increasing the volume fraction of martensite until the peak values around 50% martensite and then these mechanical properties are decreased with further increasing of martensite in the DP microstructures.

Rashid et al. [11] have studied the tempering characteristics of various DP steels particularly focusing on the microstructural changes of ferrite, martensite and retained austenite (RA) microphases, reporting that the tempering characteristics of DP steels are quite variable due to the steel chemical composition and ferrite/martensite ratio. Samuel [12] has expressed that the carbide precipitation can be occurred in the DP steel to various types and levels depending on the tempering temperature. The carbide formation starts to precipitate within martensite when the tempering temperature increases, and so the martensite becomes less hardenable, resulting lower tensile strength of DP steels [13]. Li et al. [14] has also investigated the effect of tempering on microstructural and mechanical properties of a low alloy DP steel, reporting that the tempering process resulted in the carbide precipitation and recrystallization of martensitic areas. Careful reviewing of relevant literature articles indicates that in a low alloy ferrite–martensite DP steel, the partially martensitic phase transformation can be associated with a significant level of residual stresses and high dislocation density within ferrite and martensite microphases. It is obvious that the tempering heat treatment can be used successfully to modify the strength/toughness ratio of low alloy heat treatable fully martensitic steels [15, 16]. In contrast, the effect of the tempering heat treatment on the structure-property relationships of low alloy ferrite-martensite DP steels is questionable depending on the alloying concentration, ferrite and martensite volume fractions, ferrite and martensite hardening variations, and of course the tempering heat treatment cycles [17, 18]. Therefore, the present work focuses on the effect of the tempering heat treatment on the microstructural refinements and mechanical properties of a commercial grade of 35CHGSA steel under ferrite–martensite DP condition.

2. Materials and experimental procedures

2.1. Steel chemical composition and heat treatment schedules

The steel used in this investigation was a commercial grade of hot-rolled 35CHGSA low-alloy, medium-silicon strap sample with 5mm thickness, and the chemical composition was given in Table 1. Two sets of ferrite-martensite containing samples, called fresh dual phase (FDP) and tempered dual phase (TDP) samples were prepared using the following sequential heat treatment stages: (a) all of the samples were austenitized at 900°C for 15 min and then air-cooled (normalized) to room temperature in order to develop more starting homogeneous microstructural features in the proposed heat-treated samples; (b) after reaustenitizing at 900°C for 15 min, the samples were immediately step-quenched in a molten salt bath ($1NaNO_3$ and $1KNO_3$) at 720°C and soaked isothermally for holding time of 5 min for partial decomposition of prior austenite to specific volume fraction of ferrite microconstituent following with water quenching to achieve specific volume fraction of martensite from the remaining prior metastable austenite areas, called FDP samples; and (c) tempering of second set of ferrite-martensite DP samples at 500°C for 60 min to optimize the strength–ductility properties, called TDP ones. These heat treatment cycles are shown schematically in Fig. 1.

2.2. Microstructural investigation

The metallography of heat-treated samples was carried out on the transverse section relative to hot rolling direction of as-received strap samples according to the ASTM: E3 standard [19]. The polished samples were etched with a 2% nital solution to reveal the various microstructural features. The volume fractions of ferrite and martensite microphases were measured using the point count method according to ASTM: E562 standard conditions [20]. The microstructural observations were carried out using an Olympus-PMG3 optical microscope followed with a TESCAN-MIRA 3-XMU field-emission scanning electron microscope (FE-SEM) operating at an accelerated voltage of 15 kV. The Vickers macrohardness measurements with a load of 30 kg were conducted on the heat-treated samples. The microhardness tests were also carried out at various locations within ferrite and fresh/tempered martensite microphases with a load of 5 and 10 g respectively, being applied for 20 s duration loading time using a Future Tech microhardness tester machine model FM700. The size and geometry of samples as well as the testing procedures were in accordance with ASTM: E8 (http://www.astm.org/ Standards/ E8.htm) [21] standards for tension test using an SANTAM STM-150 tension machine with an extension rate of 10 mm/min. The tensile samples were machined with a gauge length of 40 mm in such way that the applied tensile loading axis corresponded to either the rolling direction (RD) or the transverse direction (TD) of the sheet. The Charpy impact test was carried out at room temperature. Samples with a cross-section of 10 × 5 mm and a length of 55 mm were cut to perform impact tests using a Charpy impact testing machine. A 45° V notch with a 0.2 mm filet radius and a depth of 2 mm was made at the mid-point along the width of the samples. The absorbed energy was directly measured from the scale in joules. At least three samples were fractured for each condition and the mean values were calculated.

Table 1. The chemical composition of investigated low alloy medium silicon commercial grade of 35CHGSA steel (in wt%)

C	Si	Mn	P	S	Cr	Mo	Ni	Ti	V	Fe
0.35	1.25	0.89	0.01	0.01	1.18	0.01	0.04	0.03	0.01	Balance

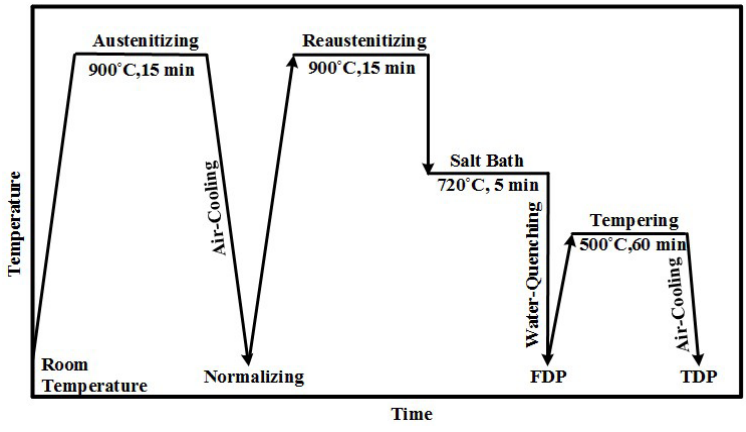

Fig. 1. Schematic diagrams indicating the heat treatment cycles used to achieve two sets of fresh and tempered ferrite-martensite DP samples. FDP: fresh dual phase; TDP: tempered dual phase.

3. Results and discussion

3.1. Microstructural observations and hardness measurements

3.1.1. Optical micrographs and hardness data

Figure 2 shows typical light micrographs of ferrite–martensite FDP and TDP marked samples in conjunction with the associated ferrite and martensite microhardness data. The microstructures of FDP and TDP samples contain the same 6% volume fraction of ferrite (light grains) with 94% volume fraction of fresh/tempered martensite (brown areas). For both sets of FDP and TDP samples, the microstructures are characterized by a mixture of ferrite and martensite microphases, with the ferritic-type microconstituent being revealed by more blocky morphology, except the packets of laths and parallel alignment of individual martensitic units are more recovered within the TDP microstructures. In this way, the ferrite, martensite, and tempered martensite microphases are indicated by F, M, and TM symbols, respectively. For more comparison, the amounts of ferrite and martensite volume fractions along with the microhardness data of ferrite and martensite microphases taken from FDP and TDP samples are given in Table 2. The average microhardness of ferrite and martensite microphases are changed from 280 to 207HV5g, and 796 to 459HV10g, with low temperature tempering heat treatment (from FDP to TDP samples), respectively. The significant lower in microhardness data of ferrite and martensite microphases for TDP samples compared to the associated FDP samples can be due to the recovery and restoration of ferrite and martensite during tempering heat treatment. The ferrite crystals in FDP samples are much harder than that of TDP ones emphasizing that the ferrite grains can be more work hardened due to the higher interaction of more carbon concentrated martensite area with the adjacent ferrite area close the ferrite-martensite interfaces [22]. The phase transformation of prior austenite to martensite causes a massive volumetric expansion of much higher than that of pure FCC to BCC iron phase transformation (8.8%), which increases the dislocation density within ferrite area adjacent to the ferrite–martensite interfaces and thus increases the hardness of ferrite grains. For this ferrite hardening mechanism, it is a well-known fact that the austenite to ferrite phase transformation has been associated with a considerable compositional changes in the ferrite and prior austenite microphases [23]. The compositional changes can be developed by long range diffusion of carbon and substitutional alloying elements in the ferrite and prior austenite areas during SQ holding at 720°C, causing a considerable higher carbon redistribution in the remaining metastable prior austenite areas adjacent to the ferrite grains. These metastable high carbon prior austenite areas can be transformed to high carbon martensite on the subsequent water quenching, generating a significant level of dislocation density within adjacent ferrite areas. On the other hand, a significant level of fine carbide precipitates can be formed during tempering at 500°C for 60 min causing the reduction in martensite tetragonality as well as lower dislocation density in the ferrite areas adjacent to ferrite–martensite interfaces [13, 24]. In fact, part of solute martensite carbon content can be associated

to the carbide precipitation, causes the lower hardness of martensite phase in the TDP samples [14, 15].

The results of Vickers macrohardness measurements for FDP and TDP samples are compared with each other in Fig. 3. The Vickers macrohardness value of 606HV30kg was related to hardening response of FDP samples, while the macrohardness of TDP ones has been significantly decreased to the number of 429HV30kg which is 177HV30kg lower than that of FDP ones. The decrease in hardness of TDP samples is in part due to the reduction in solute carbon content of martensite during tempering heat treatment, which increases the toughness and ductility of hard martensite phase. Careful investigation of ferrite and martensite microhardnesses data indicates that the ferrite hardness is also surprisingly decreased from 280 to 207HV5g which can be responsible in part to the lower hardness of TDP samples. The decrease in ferrite hardness can be fully supported by the fact that the tempering heat treatment can be related to the recovery and restoration of dislocated ferrite grains and also more drastically motivated thermally activated relaxation mechanism which reduces the accumulation of transformational residual stresses within ferrite grains adjacent to the martensite areas [13, 24].

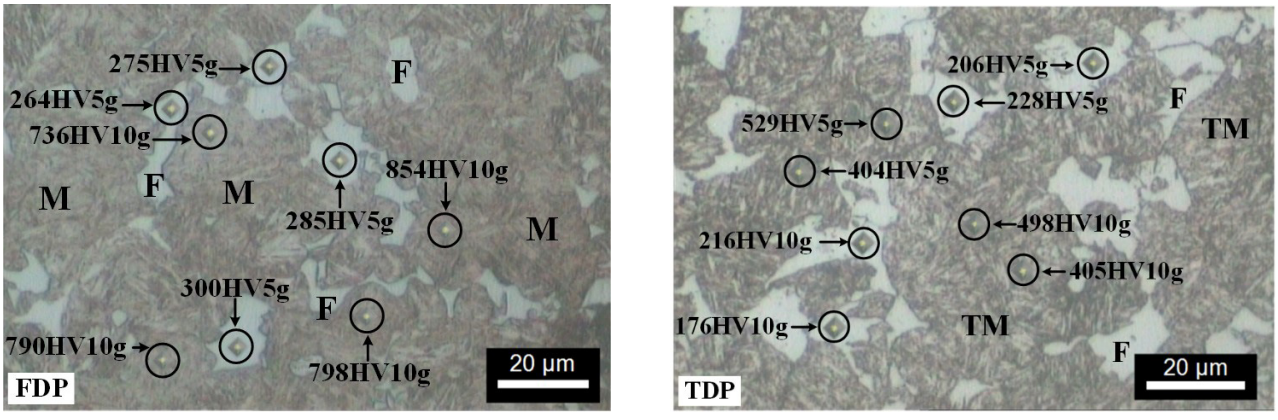

Fig. 2. Light micrographs with the associated locations and values of ferrite and martensite microhardness data taken from FDP and TDP samples. The microhardnesses measurements are associated with a constant loading force of 5g for ferrite grains and 10g for martensite and tempered martensite areas. F: Ferrite; M: Martensite; TM: Tempered Martensite.

Table 2. Characteristics of ferrite and martensite microconstituents in the FDP and TDP heat-treated samples. The samples are consisting different hardening data for ferrite and martensite microphases.

Sample mark	Ferrite volume fraction (%)	Martensite/tempered martensite volume fraction (%)	Hardness, HV30Kg	Microhardness data	
				Ferrite, HV5g	Martensite, HV10g
FDP	6	94	606	280	796
TDP	6	94	429	207	459

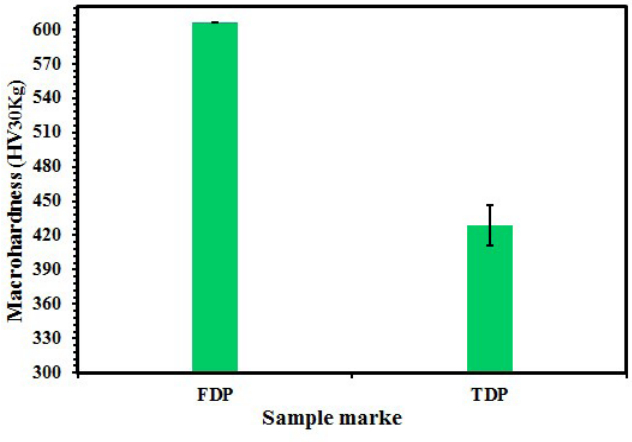

Fig. 3. The macrohardening results of ferrite–martensite FDP and TDP samples.

3.1.2. Electron micrographs

Figure 4 represents typical FE-SEM micrographs of FDP and TDP marked samples. The general features of microstructures are almost the same and that the formation of blocky shaped ferrite grains and martensitic packets are developed in the same fashion, except that the packets of martensitic crystals are more recovered and contain fine acicular carbide particles for TDP samples. Because of more diffusional rearrangement of iron and carbon atoms during tempering heat treatment, the martensitic crystals are recovered and looks like ferrite-carbide segregation. This is why in comparison to the associated light micrographs of FDP and TDP shown in Fig. 2, a good contrasting resolution can be observed between ferrite and martensite microconstituents in the tempered electron micrograph (Fig. 4, TDP). The good contracting resolution can be rationalized to the fact that these microconstituents are different in etching sensitivity causing a greater topographical contrast between tempered martensite and carbide microconstituents in relation to that of fresh ferrite and martensite microphases developed in the FDP microstructures. The FE-SEM micrographs of TDP samples deliberately confirms that a remarkable recovery and restoration of ferrite and martensite crystals are occurred in the microstructures so that the formation of fine acicular carbide particles is obvious in a relatively featureless martensitic area. Another aspect of light and electron micrographs shown in Figs. 2 and 4 is that the DP heat-treated schedule utilized in this study has been associated to the ferrite-martensite DP microstructures with alternative blocky ferrite grains surrounded with smaller packets of martensitic crystals in comparison to direct water quenched fully martensitic microstructures. This is in good agreement with the fact that for a given chemical composition of low alloy steel, the formation of different ferrite-martensite DP microstructures can be dictated by prior austenite grain boundaries from which the ferrite evolves during the soaking stage of heat treatment [25-27]. Therefore, one can expect that the recovery and restoration of more defected ferrite and martensite microphases carbon occurred in the TDP microstructures. Of course, two factors of carbide precipitation into the dislocation and reduction of residual stresses by lower tetragonality of martensite during tempering heat treatment are also consequential variable parameters of tempering process [28].

3.2. Mechanical properties

3.2.1. Tensile behavior

Typical engineering stress-engineering strain curves corresponding to the ferrite-martensite FDP and TDP samples are shown in Fig. 5, and so the corresponding tensile properties have been also summarized in Table 3. The FDP samples were related to a general brittle mechanical behavior, in which these samples showed the ultra-high yield strength (YS) and ultimate tensile strength (UTS) of 1290 and 1353MPa, respectively, in conjunction with low value of 1.8% uniform elongation (UE). By tempering heat treatment, the most of thermal and phase transformational residual stresses were relieved, and the ferrite and martensite microphases were softened. Therefore, the YS and UTS were decreased to values of 960 and 1071MPa, while UE and Total Elongation (TE) were significantly increased to 8.9 and 14.8% for the TDP

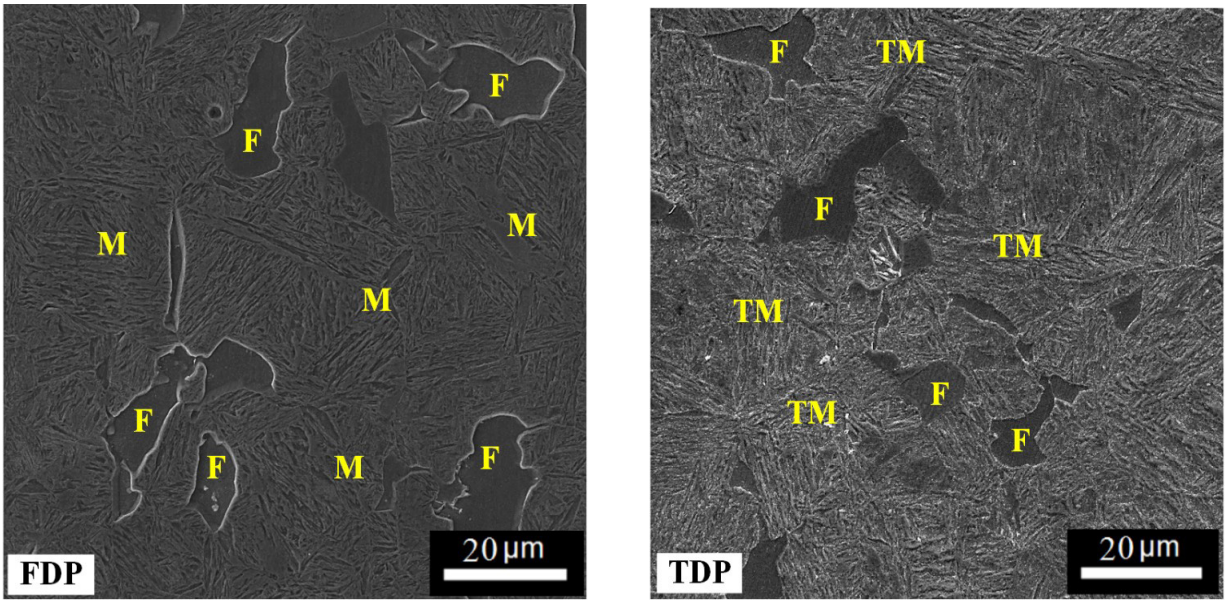

Fig. 4. Selected FE-SEM micrographs of FDP and TDP heat-treated samples. The tempering heat treatment was carried out at 500°C for 60 min for ferrite–martensite TDP marked samples. Ferrite grains, martensite and tempered martensite regions are labeled as F, M and TM symbols, respectively.

marked samples, respectively. Moreover, the strength difference between FDP and TDP marked samples was only 282MPa (from 1353 to 1071MPa, respectively). In fact, with tempering heat treatment, two independently phenomena can be occurred in the ferrite-martensite DP microstructures. One is that the carbon concentration of martensite decreases due to the carbide precipitation [29], causing lower strength with higher ductility of martensitic microconstituent. The other phenomenon is the recovery and restoration of ferrite grains as a consequence of lower ferrite microhardness in the TDP samples. The ferrite microhardness has been significantly decreased from 280 to 207HV5g emphasizing that the ferrite grains are associated with lower dislocation density.

For more information, the comparison of TE multiple UTS data for FDP and TDP samples are shown in Fig. 6 with the other literature reported results for investigated advanced high strength steel grades. It can be observed that the tensile properties of TDP marked samples are much higher than the other advanced high strength steel grades. More importantly, despite the lower level of YS for TDP samples compared to FDP ones (Fig. 5, Table 3), the combination of higher strength with good ductility has been achieved for TDP samples (Fig. 6). These results indicate that the TDP samples have an optimum level of tensile properties compared to the other investigated advanced high strength steels, so that the product of TE multiple UTS is significantly increased to the higher value of 15.8% GPa (Table 3). Light and electron microstructural observations show that the fresh martensitic microconstituent formed in the ferrite-martensite DP samples leads to a high level of strength with relatively low elongation (Figs. 2, 4, Table 3). With low temperature tempering of DP samples, the microhardness of martensite reduces considerably, while the reduction in ferrite microhardness is moderately causing the lower difference between ferrite and martensite microhardness data in the TDP samples. It is evident that their softening of martensite reduces the strength because the strength of FDP samples is mainly determined by the strength of hard martensite microconstituent. On the other hand, when the hardness of martensite decreases, the ductility of TDP samples increases significantly. The brittle behavior of FDP microstructures can be due to the propagation of crack in the brittle martensitic matrix causing sudden failure in the early stage of plastic deformation. The tempering heat treatment has been associated with the formation of carbide precipitation within martensite resulting in the lower tetragonality of brittle martensite microconstituent. On the other hand, the dislocation generated within martensite by displacive martensitic phase transformation is a suitable place for carbide precipitation. With the formation of these particles, the number of free dislocation ferrite and martensite microphases is reduced and therefore the propagation of crack is retarded, causing a ductile fracture in TDP samples [13].

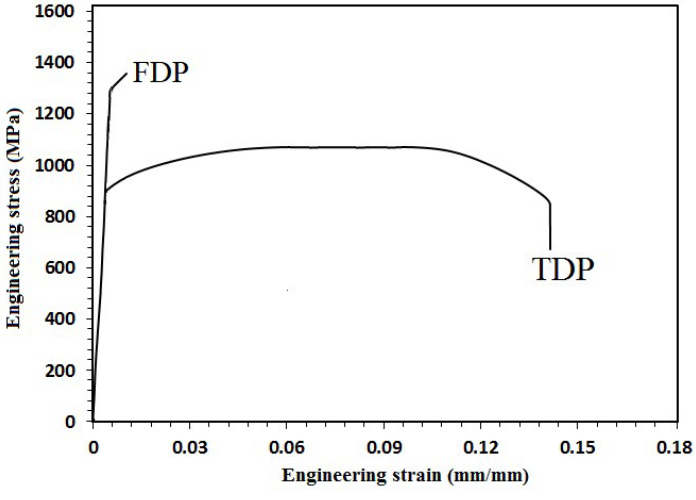

Fig. 5. The engineering stress-engineering strain curves of ferrite-martensite FDP and TDP samples.

Table 3. The average tensile properties of ferrite-martensite FDP and TDP samples. The symbols of YS, UTS, UE, TE and PSE are corresponding to yield strength, ultimate tensile strength, uniform elongation, total elongation and the product of tensile strength multiple total elongation, respectively.

Sample mark	YS, MPa	UTS, MPa	UE, %	TE, %	PSE, GPa. %
FDP	1290	1353	1.8	1.8	2.4
TDP	960	1071	8.9	14.8	15.8

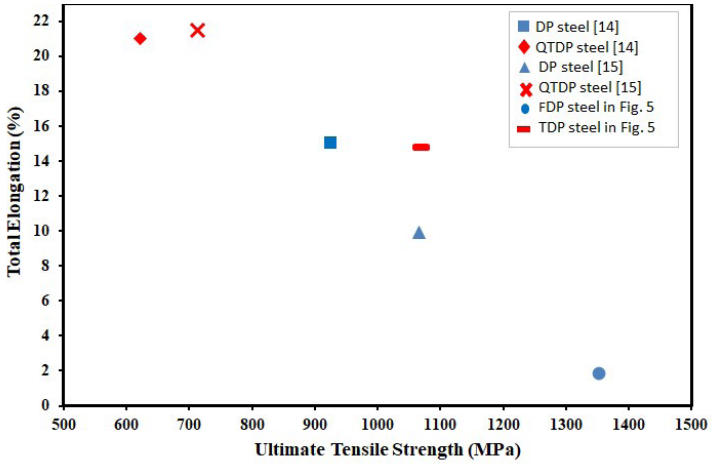

Fig. 6. The comparison between tensile properties of FDP and TDP samples in conjunction with the other literature reported data for advanced high strength steel grades [14, 15]. The TE and UTS are selected to illustrate the ductility and strength of advanced high strength steels.

3.2.2. Toughness characteristics

The comparison of absorbed impact energy between ferrite-martensite FDP and TDP samples has been illustrated in Fig. 7. Accordingly, there is a significant difference between absorbed impact energy of FDP with TDP samples. For almost a 50% loss in hardness level from FDP to TDP samples, the absorbed impact energy is sharply increased from 3.5 to 12 J (about four limes) corresponding to the impact properties of FDP and TDP marked samples, respectively. These results are consistent with the literature reporting data indicating that the elongation and absorbed impact energy are increased with tempering of fully martensitic low alloy heat treatable steels [14, 15]. A ductile matrix phase (ferrite) in conjunction with a moderately hard phase tempered (martensite) can play the stress relaxation role to the crack tip, and consequently the crack propagation can be retarded resulting in a higher combination of elongation with absorbed impact energy for TDP samples in comparison with that of FDP ones [15, 30, 31], although the solubility of more than 0.5 wt% of silicon in the investigated low alloy steel can be related in part to the lower impact properties [32]. Moreover, as shown in Fig. 2, the ferrite microhardness for FDP samples is significantly higher than that of TDP ones. Emphasizing that, the slip bands and crack propagation can be accelerated within the hard ferrite grains in the FDP samples. Purring low temperature tempering heat treatment, the multivariant carbide particles are formed perpendicular to the crack growth direction causing lower crack propagation within tempered martensite areas [36]. Moreover, in the TDP samples, due to the reduction in martensite tetragonality resulting from tempering heat treatment and also the reduction in ferrite microhardness, a higher cooperative plastic deformation behavior of ferrite and martensite microphases can be developed within the microstructures causing a higher absorbed impact energy for TDP samples.

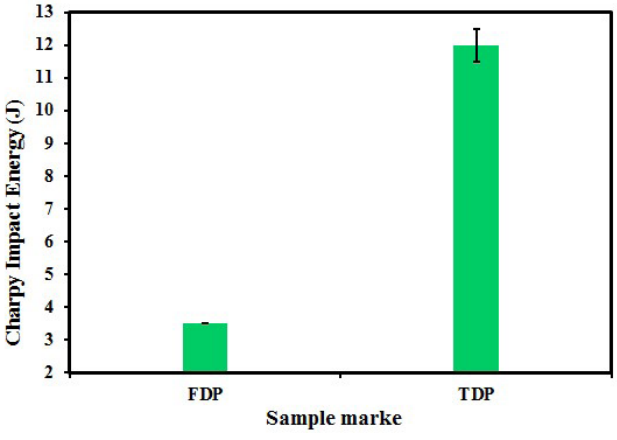

Fig. 7. The comparison between Charpy absorbed impact energy of ferrite-martensite FDP and TDP samples.

3.2.3. Work hardening behavior

For interpreting the work hardening behavior of ferrite-martensite FDP and TDP microstructures, it is significant to address the deformation response of individual ferrite and martensite microconstituents formed in the samples. In this way, the work-hardening behavior of tensile tested samples was analyzed using the well-known Holloman equation [33] in its logarithmic form as following:

$$Ln(\sigma) = nLn(\varepsilon) + Ln(K) \quad (1)$$

where σ, ε, n, and K symbols are corresponding to the true stress, true strain, strain-hardening exponent, and strength coefficient, respectively. In this way, the value of strain hardening exponent "n" has been used to compare

the work hardening behavior of FDP and TDP samples. The higher value of "n" is corresponding to the higher work hardening and more plastic deformation before necking condition. By plotting the true stress–strain data for the range of uniform plastic deformation in a logarithmic scale, and fitting a linear relationship between these data, the corresponding strain-hardening exponent and strength coefficient can be obtained. Accordingly, Fig. 8 illustrates typical plots of Eq. (1) for the tensile data, and so the associated mean values of strain-hardening exponent and strength coefficient are given in Table 4. The plastic deformation response and the corresponding work-hardening indices of tensile tested samples can be also examined through the comparative changes in the amounts of YS and UTS values (i.e., the yield ratio) [34], and so the data of yield ratio are given in Table 4. These results indicate that the FDP samples illustrated a single stage of work-hardening pattern, while the TDP samples are associated with a double stage of work-hardening pattern. An amount of 0.078 for strain-hardening exponent with 1883MPa strength coefficient have been accompanied with an amount of 0.95 yield ratio for FDP samples. In contrast, the doublet stage of work-hardening is due to the difference in the plastic deformation of soft ferrite phase with hard-tempered martensite in the TDP microstructures. The first stage of work-hardening is related to the plastic deformation of soft ferrite grains and the second stage corresponding to the simultaneous plastic deformation of soft ferrite with hard-tempered martensite microphases. In other words, the ferrite-tempered martensite microstructures resulting from TDP heat treatment process show a double stage of plastic deformation behavior in which for the first stage of plastic deformation, the applied stress is somewhat higher than the YS of soft ferrite grains, but less than the YS of hard-tempered martensite phase. Therefore, the ferrite phase in the form of plastic deformation and tempered martensite in the form of elastic deform are both code-formed in the first stage of the work hardening pattern, while in the second stage of work-hardening, both soft ferrite and hard-tempered martensite phases are code-formed plastically in the TDP microstructures. These claims are rationalized by the fact that the TDP samples illustrated higher strain-hardening exponents in the first stage of plastic deformation (0.092) in comparison to the lower strain-hardening exponent if second stage (0.050) with the associated lower yield ratio of 0.89 compared to the FDP tensile tested samples. Moreover, the amount of "K" has been significantly decreased from 1883 to 1248MPa for first stage of work-hardening with tempering treatment. Therefore, the observed higher YS and UTS of FDP samples in comparison with TDP ones can be related to the lower work hardening behavior of fresh ferrite and martensite microphases.

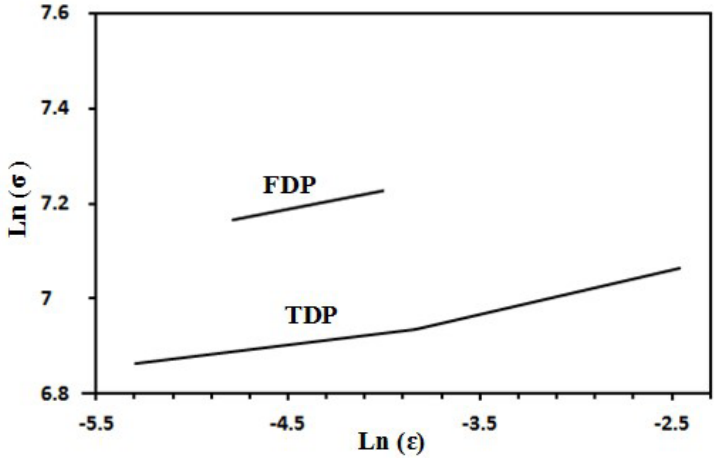

Fig. 8. The logarithmic plots of Holloman equation applied to the tensile tested stress-strain data of FDP and TDP samples.

Table 4. The average values of strain-hardening exponent (n) and strength coefficient (K) of work hardening pattern association with the yield ratio of tensile tested samples.

Sample mark	Stage I		Stage II		Yield ratio
	n	K (MPa)	n	K (MPa)	
FDP	0.078	1883	-	-	0.95
TDP	0.092	1248	0.050	1466	0.89

4. Conclusions

In the present research work, effect of low temperature tempering heat treatment on the microstructures and mechanical properties of a commercial grade of medium silicon low alloy 35CHGSA steel under ferrite-martensite DP microstructres has been investigated. The following conclusions have been obtained:

- The ferrite and martensite morphologies and volume fractions are the same in both of ferrite–martensite FDP and TDP microstructures. The microstructures are characterized by a mixture of ferrite and martensite microphases, with the ferritic-type microconstituent being revealed by blocky morphology.
- The ferrite and martensite hardness data are quite variable in the ferrite–martensite FDP and TDP samples. The average microhardness of ferrite has been surprisingly decreased from 280 to 207HV5g corresponding to the FDP and TDP hardness data, respectively. The martensite microhardness has been also decreased from 796 to 459HV10g after low temperature tempering heat treatment of FDP samples.
- The tensile properties of TDP heat-treated samples are significantly increased compared to that of FDP ones. The product of tensile strength multiple total elongation of FDP samples is 1.8% GPa, while this value is significantly increased to 14.8% GPa for TDP samples.
- The difference between ferrite and martensite microhardness data are significantly decreased from 516 to 252HV corresponding to the FDP and TDP samples, respectively. The low difference between ferrite and tempered martensite hardness data in TDP samples causes ferrite and tempered martensite microphases are both codeformed plastically, while the ferrite has been independently deformed plastically in FDP samples.
- The low value of 3.5 J absorbed impact energy has been related to FDP samples, while the TDP heat-treated ones are associated with the value of 12 J absorbed impact energy, about four times higher if being compared to that of FDP ones.
- The work-hardening behavior of TDP samples is characterized by a double stage of pattern, while the work-hardening of FDP ones is linearly involved a single-stage of pattern. The strain hardening exponent for the first stage of work-hardening in TDP samples (0.092) is more than that of FDP ones (0.078), while the trend in strength coefficient is vice versace. The strength coefficient of FDP samples (1883MPa) is more than the TDP ones (1248MPa).

References

[1] T. Baudin, C. Quesne, J. Jura, R. Penelle, Microstructural characterization in a hot-rolled, two-phase steel, Materials characterization. 47 (2001) 365-373. https://doi.org/10.1016/S1044-5803(02)00183-3.

[2] E. Ahmad, T. Manzoor, K.L. Ali, J. Akhter, Effect of microvoid formation on the tensile properties of dual-phase steel, Journal of materials engineering and performance. 9 (2000) 306-310. https://doi.org/10.1361/105994900770345962.

[3] E. Ahmad, R. Priestner, Effect of rolling in the intercritical region on the tensile properties of dual-phase steel, Journal of materials engineering and performance. 7 (1998) 772-776. https://doi.org/10.1361/105994998770347341.

[4] H.R.K. Zarchi, A. Khajesarvi, S.S.G. Banadkouki, M.C. Somani, Microstructural evolution and carbon partitioning in interstitial free weld simulated APIX60 steel, Reviews on Advanced Materials Science. 58 (2019) 206-217. https://doi.org/10.1515/rams-2019-0016.

[5] S.G. Banadkouki, E. Fereiduni, Effect of prior austenite carbon partitioning on martensite hardening variation in a low alloy ferrite–martensite dual phase steel, Materials Science and Engineering: A. 619 (2014) 129-136. https://doi.org/10.1016/j.msea.2014.09.041.

[6] O. Abedini, M. Behroozi, P. Marashi, E. Ranjbarnodeh, M. Pouranvari, Intercritical Heat Treatment Temperature Dependence of Mechanical Properties and Corrosion Resistance of Dual Phase Steel, Materials Research. 22 (2019). https://doi.org/10.1590/1980-5373-MR-2017-0969.

[7] M. Alipour, M.A. Torabi, M. Sareban, H. Lashini, E. Sadeghi, A. Fazaeli, M. Habibi, R. Hashemi, Finite element and experimental method for analyzing the effects of martensite morphologies on the formability of DP steels, Mechanics Based Design of Structures and Machines. (2019) 1-17. https://doi.org/10.1080/15397734.2019.1633343.

[8] B. Sunil, S. Rajanna, Evaluation of mechanical properties of ferrite-martensite DP steels produced through intermediate quenching technique, SN Applied Sciences. 2 (2020) 1-8. https://doi.org/10.1007/s42452-020-03246-4.

[9] P. Huyghe, L. Malet, M. Caruso, C. Georges, S. Godet, On the relationship between the multiphase microstructure and the mechanical properties of a 0.2 C quenched and partitioned steel, Materials Science and Engineering: A. 701 (2017) 254-263. https://doi.org/10.1016/j.msea.2017.06.058.

[10] P. Movahed, S. Kolahgar, S. Marashi, M. Pouranvari, N. Parvin, The effect of intercritical heat treatment temperature on the tensile properties and work hardening behavior of ferrite–martensite dual phase steel sheets, Materials Science and Engineering: A. 518 (2009) 1-6. https://doi.org/10.1016/j.msea.2009.05.046.

[11] M. Rashid, B. Rao, Tempering characteristics of a vanadium containing dual phase steel, Metallurgical transactions A. 13 (1982) 1679-1686. https://doi.org/10.1007/BF02647823.

[12] F. Samuel, Effect of dual-phase treatment and tempering on the microstructure and mechanical properties of a high strength, low alloy steel, Materials Science and Engineering. 75 (1985) 51-66. https://doi.org/10.1016/0025-5416(85)90177-6.
[13] X. Fang, Z. Fan, B. Ralph, P. Evans, R. Underhill, Effects of tempering temperature on tensile and hole expansion properties of a C–Mn steel, Journal of materials processing technology. 132 (2003) 215-218. https://doi.org/10.1016/S0924-0136(02)00923-8.
[14] H. Li, S. Gao, Y. Tian, D. Terada, A. Shibata, N. Tsuji, Influence of tempering on mechanical properties of ferrite and martensite dual phase steel, Materials Today: Proceedings. 2 (2015) 667-671. https://doi.org/10.1016/j.matpr.2015.07.372.
[15] A.A. Sayed, S. Kheirandish, Affect of the tempering temperature on the microstructure and mechanical properties of dual phase steels, Materials Science and Engineering: A. 532 (2012) 21-25. https://doi.org/10.1016/j.msea.2011.10.056.
[16] A. Kamp, S. Celotto, D. Hanlon, Effects of tempering on the mechanical properties of high strength dual-phase steels, Materials Science and Engineering: A. 538 (2012) 35-41. https://doi.org/10.1016/j.msea.2012.01.008.
[17] M. Erdogan, R. Priestner, Effect of martensite content, its dispersion, and epitaxial ferrite content on Bauschinger behaviour of dual phase steel, Materials science and technology. 18 (2002) 369-376. https://doi.org/10.1179/026708302225001679.
[18] A. Joarder, J. Ojha, D. Sarma, The tempering behavior of a plain carbon dual-phase steel, Mater, Charact. 25 (1990) 9-209. https://doi.org/10.1016/1044-5803(90)90010-H.
[19] A. Norma, E3-01, Standard Guide for Preparation of metallographic specimens, American Society for Testing and Materials ASTM International, West Conshohocken, PA.
[20] P. Fazio, Annual Book of ASTM Standards, Philadelphia, Pa.: American Society for Testing Materials, 1993.
[21] A. Kardak, L. Bilich, G. Sinclair, Stress concentration factors for ASTM E8/E8M-15a plate-type specimens for tension testing, Journal of Testing and Evaluation. 45 (2017) 2294-2298.
[22] A. Khajesarvi, S.G. Banadkouki, Investigation of carbon and silicon partitioning on ferrite hardening in a medium silicon low alloy ferrite-martensite dual-phase steel. 17 (2020), 25-33. https://dx.doi.org/10.22034/ijissi.2021.527641.1189.
[23] E. Fereiduni, S.G. Banadkouki, Improvement of mechanical properties in a dual-phase ferrite–martensite AISI4140 steel under tough-strong ferrite formation, Materials & Design. 56 (2014) 232-240. https://doi.org/10.1016/j.matdes.2013.11.005.
[24] M.S. Htun, S.T. Kyaw, K.T. Lwin, Effect of heat treatment on microstructures and mechanical properties of spring steel, Journal of metals, materials and minerals. 18 (2008) 191-197.
[25] D. Das, P.P. Chattopadhyay, Influence of martensite morphology on the work-hardening behavior of high strength ferrite–martensite dual-phase steel, Journal of materials science. 44 (2009) 2957-2965. https://doi.org/10.1007/s10853-009-3392-0.
[26] A. Bag, K. Ray, E. Dwarakadasa, Influence of martensite content and morphology on tensile and impact properties of high-martensite dual-phase steels, Metallurgical and Materials Transactions. A 30 (1999) 1193-1202. https://doi.org/10.1007/s11661-999-0269-4.
[27] A. Ebrahimian, S.G. Banadkouki, Effect of alloying element partitioning on ferrite hardening in a low alloy ferrite-martensite dual phase steel, Materials Science and Engineering: A. 677 (2016) 281-289. https://doi.org/10.1016/j.msea.2016.09.073.
[28] R. Davies, R. Kot, B. Bramfitt, Fundamentals of dual phase steels, Conference proceedings (Metallurgical society of AIME), 1981, pp. 265-277.
[29] R.W.K. Honeycombe, Steels microstructure and properties, Metallurgy and materials science. 1 (1995).
[30] A.S. Ghorabaei, S.G. Banadkouki, Abnormal Mechanical Behavior of a Medium-Carbon Steel under Strong Ferrite-Pearlite-Martensite Triple-Phase Microstructures, Materials Science and Engineering: A. (2017). https://doi.org/10.1016/j.msea.2017.06.035.
[31] Y. Liu, D. Fan, S.P. Bhat, A. Srivastava, Ductile fracture of dual-phase steel sheets under bending, International Journal of Plasticity. 125 (2020) 80-96. https://doi.org/10.1016/j.ijplas.2019.08.019.
[32] F. Sorbello, P. Flewitt, G. Smith, A. Crocker, The role of deformation twins in brittle crack propagation in iron–silicon steel, Acta Materialia. 57 (2009) 2646-2656. https://doi.org/10.1016/j.actamat.2009.02.011.
[33] G.E. Dieter, D.J. Bacon, Mechanical metallurgy, McGraw-hill New York 1976.
[34] H. Beladi, I. Timokhina, X.-Y. Xiong, P.D. Hodgson, A novel thermomechanical approach to produce a fine ferrite and low-temperature bainitic composite microstructure, Acta materialia. 61 (2013) 7240-7250. https://doi.org/10.1016/j.actamat.2013.08.029.